

A Stochastic Multi-Objective Optimization Framework for Planning and Scheduling of Community Energy Storage Systems

K.B.J. Anuradha, *Student Member, IEEE*, and Chathurika P. Mediwaththe, *Member, IEEE*

Abstract—This paper explores a methodology to optimize the planning and the scheduling of a community energy storage (CES) considering the uncertainty of real power consumption and solar photovoltaic (SPV) generation of the customers in low voltage (LV) distribution networks. To this end, we develop a stochastic multi-objective optimization framework which minimizes the investment and the operation costs of the CES provider, and the social costs of the customers (i.e. cost of customers for trading energy with the grid and the CES). The uncertainty of SPV generation and real power consumption are modelled to follow the beta and normal distributions, respectively. Then, the roulette wheel mechanism (RWM) is exploited to formulate a scenario-based stochastic program. The initial scenarios obtained from the RWM, are then reduced by using the K-Means clustering algorithm, to keep the problem tractability. A case study highlights our model provides 10-21% more cumulative economic benefits for the customers and the CES provider, compared with the models that optimize only the CES scheduling. Also, the simulation results for different energy price schemes of the CES provider reflect, the customers change their power exchange with the CES and the grid significantly, to minimize their social costs.

Index Terms—Community energy storage (CES), multi-objective optimization, planning and scheduling, power flow, roulette wheel mechanism (RWM), scenarios, uncertainty

I. INTRODUCTION

THE integration of solar photovoltaic (SPV) systems in low voltage (LV) distribution networks, has undergone a rapid upsurge over the last few decades. However, the intermittent and non-dispatchable nature of SPV generation, may restrict their beneficiaries such as the customers from exploiting the merits of SPV fully. These issues can be efficiently alleviated by exploiting energy storage systems. Community energy storage (CES) devices are an emerging type of battery system, which is gaining increasing interest in the industry, as they can enable increased community access and network hosting capacity for renewable energy [1].

An energy management framework which aims at optimizing only the scheduling of a CES such as its charging and discharging pattern, may not deliver the expected rewards from a CES completely. Hence, it is imperative that the planning aspects including the location, the capacity and the rated power of a CES are optimized concurrently with its

scheduling. Several studies have presented deterministic optimization frameworks to find the optimal CES planning and/or the scheduling, and thus achieve the objectives of different stakeholders [2]–[4]. Here, the authors have assumed both real power consumption and SPV generation of the customers are perfectly known ahead from their forecasts. However, due to the uncertainty of SPV generation and real power consumption of the customers, their forecast errors can be quite high at times. Eventually, this may result the optimization models described in [2]–[4] unable to achieve the objectives effectively. Also, different stakeholders have distinct objectives for them. Thus, a multi-objective optimization framework can reflect the trade-offs between those objectives comprehensively.

In this paper, we examine the extent to which the optimal planning and scheduling of a CES benefit different stakeholders. To this end, we develop an energy management framework between the customers, the CES and the grid, by incorporating the uncertainty of real power consumption and SPV generation of the customers. Additionally, we leverage a linearized power flow model with our energy management framework to formulate a mixed integer linear program (MILP). In summary, the main contributions of this paper can be highlighted as follows.

- We develop a stochastic multi-objective optimization framework which optimizes both planning and scheduling of a CES for benefiting (i) the CES provider by minimizing the investment and the operation costs of the CES, and (ii) the customers by minimizing their social costs.
- The proposed optimization framework is capable of providing significantly higher economic benefits for the CES provider and the customers than in the models which arbitrarily choose the CES connected node.
- A case study compares our proposed stochastic model with its corresponding deterministic model for different energy price schemes of the CES provider. This study enables to understand how the economic benefits for the CES provider, and for the customers change due to the uncertainty of real power consumption and SPV generation of the customers, and the energy price scheme of the CES provider.

Prior research work have presented optimization frameworks which focus on the scheduling of the CES [2], [3], and both planning and scheduling of CES [4]–[7]. For instance, the authors of [2] have presented a method for CES scheduling, to minimize the social costs of the customers while maximizing the revenue of the CES provider. In [3], an optimization

K. B. J. Anuradha is with The Australian National University, Canberra, ACT 0200, Australia (email: u7146121@anu.edu.au).

Chathurika P. Mediwaththe is with The Australian National University, Canberra, ACT 0200, Australia, and also with the Commonwealth Scientific and Industrial Research Organisation, Canberra, ACT 2601, Australia (email: chathurika.mediawaththe@csiro.au).

framework is presented to schedule the CES, to minimize the real energy losses, and energy trading costs with the grid by the CES provider and the customers. The authors of [4] and [5] have presented models to optimize the CES planning and scheduling simultaneously, to enhance the hosting capacity of LV networks, and to mitigate the voltage excursions in three phase unbalanced LV networks, respectively. Also, analytical methods for optimizing the CES planning and scheduling have been discussed in [6], [7]. A common feature of [2]–[7] is that the authors have used deterministic models, assuming the SPV generation and the real power consumption of the customers are known ahead with no uncertainty. Hence, those models may not be efficient in providing realistic planning and operation decisions.

The uncertainty of real power consumption and generation from SPV have been taken into account in [8], [9] for CES management problems. For instance, the authors of [8] have presented a method for optimizing both planning and scheduling of CES to accomplish multiple objectives. Here, the authors have used the normal distribution and the RWM to model the uncertainty of real power consumption and SPV generation. In [9], the authors of have investigated how the CES location impacts the voltage profile and real power losses in LV networks. For this, they have arbitrarily allocated the CES at different nodes. In contrast to [2]–[7], our paper optimizes both planning and scheduling aspects of the CES taking into account the uncertainty of real power consumption and SPV generation. Thus, our approach models the CES planning and its scheduling problem more realistically. Also, compared to [8], [9], we present a method to minimize the personal costs of the CES provider and the customers concurrently.

This paper is structured as follows. Notations used in this paper are detailed in Section II. The system models of the CES, the customers and the network power flow are presented in Section III. The stochastic models of SPV generation and real power consumption of the customers are given in Section IV. The formulation of the multi-objective optimization framework is described in Section V. Section VI presents the validation of the results, and Section VII gives the conclusion of the paper.

II. NOTATIONS

A. Stochastic Model-related Notations

To formulate a scenario-based stochastic program, the uncertainty of SPV generation and real power consumption of the customers are modelled using known probability density functions. Here, a scenario represents a possible combination of SPV generation and real power consumption of all the customers together with their corresponding probabilities at a given time. The initial set of scenarios is denoted by \mathcal{R} , and $r \in \mathcal{R}$. Due to the computational complexity of stochastic programs which use scenarios, it is imperative to use a scenario reduction approach to reduce the number of scenarios, and keep the problem tractability. Thus, a scenario reduction technique is used in this paper, and the set composed by the reduced scenarios is given by \mathcal{S} , where $s \in \mathcal{S}$. The implementation of the scenario-based stochastic program including the scenario reduction are discussed in Section IV.

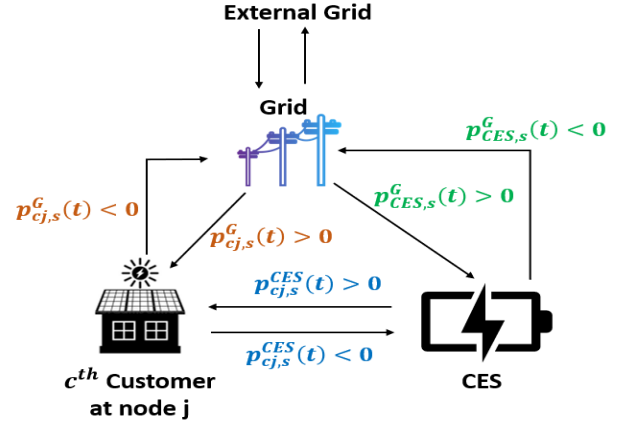


Fig. 1: Mutual power exchanges between the CES, the grid and a customer in scenario s at time t

B. Network and Power Flow-related Notations

In this paper, a distribution network with a radial topology is considered. It is described by the graph $\mathcal{G} = (\mathcal{V}, \mathcal{E})$, where $\mathcal{V} = \{0, 1, \dots, N\}$ is the set of all nodes, and $\mathcal{E} = \{(i, j)\} \subset \mathcal{V} \times \mathcal{V}$ is the set of all lines in the network. Node 0 (slack node) represents the secondary side of the distribution transformer. The resistance and the reactance of line (i, j) are r_{ij} (in Ω) and x_{ij} (in Ω), respectively. The set of customers at node j is represented by \mathcal{C}_j , and $c \in \mathcal{C}_j \forall j \in \mathcal{V} \setminus \{0\}$. Also, $t \in \mathcal{T}$, where \mathcal{T} is the set of time intervals, and Δt is the difference between two adjacent time instances (in hours). The real and reactive power flow from i to j node in scenario s at time t are represented by $P_{ij,s}(t)$ (in kW) and $Q_{ij,s}(t)$ (in kVAR), respectively. Also, $\forall j \in \mathcal{V} \setminus \{0\}, t \in \mathcal{T}, s \in \mathcal{S}$, the real power absorption, reactive power absorption, voltage and squared voltage are given by $p_{j,s}(t)$ (in kW), $q_{j,s}(t)$ (in kVAR), $V_{j,s}(t)$ (in V) and $U_{j,s}(t)$ (in V^2), respectively.

III. SYSTEM MODELS

This section first presents the network power flow model, followed by the power exchange model of the customers, and the CES model. We consider each customer, the CES and the grid can exchange power with each entity as shown in Fig. 1.

A. Power Flow Model of the Network

In this work, we consider the power absorption for the nodes as positive, and the power injections from the nodes as negative. Additionally, it is considered that there are multiple customers at each node. To model the network power flows, we use the linearized power flow equations (1) and (2) from the Distflow model in [10].

$$P_{ij,s}(t) = p_{j,s}(t) + \sum_{k:j \rightarrow k} P_{jk,s}(t) \quad \forall (i, j) \in \mathcal{E}, t \in \mathcal{T}, s \in \mathcal{S} \quad (1)$$

$$Q_{ij,s}(t) = q_{j,s}(t) + \sum_{k:j \rightarrow k} Q_{jk,s}(t) \quad \forall (i, j) \in \mathcal{E}, t \in \mathcal{T}, s \in \mathcal{S} \quad (2)$$

The real and reactive power absorbed by the node j at time t in scenario s , can be expressed as (3) and (4). The real power absorption for the CES installed node is governed by (3a), while for all the other nodes (except slack node), it is (3b). The equation (4) handles the reactive power absorption for all nodes, and we assume the CES and the SPV devices operate at unity power factor. The real power consumption, reactive power consumption and SPV generation of the customer c at node j at time t in scenario s are given by $p_{cj,s}^L(t)$ (in kW), $q_{cj,s}^L(t)$ (in kVAR) and $p_{cj,s}^{PV}(t)$ (in kW), respectively. For $j \in \mathcal{V} \setminus \{0\}$, $t \in \mathcal{T}$, $s \in \mathcal{S}$, the CES charging and discharging power are represented by $p_{j,s}^{CES,ch}(t)$ and $p_{j,s}^{CES,dis}(t)$, respectively.

$$p_{j,s}(t) = \sum_{c \in C_j} p_{cj,s}^L(t) - \sum_{c \in C_j} p_{cj,s}^{PV}(t) + p_{j,s}^{CES,ch}(t) - p_{j,s}^{CES,dis}(t) \quad (3a)$$

$$p_{j,s}(t) = \sum_{c \in C_j} p_{cj,s}^L(t) - \sum_{c \in C_j} p_{cj,s}^{PV}(t) \quad \forall j \in \mathcal{V} \setminus \{0\}, t \in \mathcal{T}, s \in \mathcal{S} \quad (3b)$$

$$q_{j,s}(t) = \sum_{c \in C_j} q_{cj,s}^L(t) \quad \forall j \in \mathcal{V} \setminus \{0\}, t \in \mathcal{T}, s \in \mathcal{S} \quad (4)$$

The linearized Distflow equations described in (1)-(2) can be explicitly written as (5), where $U_0 = |V_0|^2$ and $\mathbf{U} = |\mathbf{V}(t)|^2$ are the vectors of the squared voltage magnitude of the slack node, and the squared voltage magnitudes of all other nodes, respectively. $\mathbf{1}$ symbolizes a vector of all ones. Moreover, \mathbf{p} and \mathbf{q} are the vectors of real and reactive power absorption at each node. The matrices $\tilde{\mathbf{R}}$ and $\tilde{\mathbf{X}} \in \mathbb{R}^{N \times N}$ have the elements $R_{ij} = 2 \sum_{(m,n) \in L_i \cap L_j} r_{mn}$ and $X_{ij} = 2 \sum_{(m,n) \in L_i \cap L_j} x_{mn}$, respectively, where L_i is the set of lines on the path which connects node 0 and i [2], [10]. Also, (6) ensures the squared voltage magnitude at each node is within its allowable voltage magnitude limits. Here, $\mathbf{U}_{\min} = |V_{\min}^2| \mathbf{1}$ and $\mathbf{U}_{\max} = |V_{\max}^2| \mathbf{1}$, where V_{\min} and V_{\max} are the allowable lower and upper bound of voltage, respectively.

$$\mathbf{U} = U_0 \mathbf{1} - \tilde{\mathbf{R}} \mathbf{p} - \tilde{\mathbf{X}} \mathbf{q} \quad \forall t \in \mathcal{T}, s \in \mathcal{S} \quad (5)$$

$$\mathbf{U}_{\min} \leq \mathbf{U} \leq \mathbf{U}_{\max} \quad \forall t \in \mathcal{T}, s \in \mathcal{S} \quad (6)$$

B. Power Exchange Model of the Customers

According to Fig. 1, $p_{cj,s}^G(t)$ and $p_{cj,s}^{CES}(t)$ denote the real power exchange with the grid and the CES by the customer c at node j at time t in scenario s , respectively. When $p_{cj,s}^G(t) > 0$, it suggests a power import from the grid by a customer. On the contrary, when that customer exports power back to the grid, it will be $p_{cj,s}^G(t) < 0$. The same sign convention is used for customer power exchanges with the CES, and CES power exchange with the grid $p_{CES,s}^G(t)$ (in kW).

When a customer's SPV generation is insufficient to fulfill its real power consumption, that deficit is attained by importing power from the grid and the CES. This is mathematically

represented by (7a). Nevertheless, the imported power from each entity should be within the deficit quantity. This is ensured by (7b) and (7c). Besides, when that customer has excess SPV generation, it exports its surplus to the grid and the CES, which is mathematically interpreted by (8a). Similar to (7b) and (7c), the exported power to the CES and the grid should not exceed the mismatch of the SPV generation and the real power consumption. This is demonstrated by (8b) and (8c). Considering the ability of the CES to exchange power with the grid and the customers, $p_{CES,s}^G(t)$ can be expressed in terms of $p_{cj,s}^{CES}$, $p_{j,s}^{CES,ch}(t)$ and $p_{j,s}^{CES,dis}(t)$ as in (9).

If $p_{cj,s}^L(t) \geq p_{cj,s}^{PV}(t)$:

$$0 \leq p_{cj,s}^G(t) + p_{cj,s}^{CES}(t) = p_{cj,s}^L(t) - p_{cj,s}^{PV}(t) \quad (7a)$$

$$0 \leq p_{cj,s}^G(t) \leq p_{cj,s}^L(t) - p_{cj,s}^{PV}(t) \quad (7b)$$

$$0 \leq p_{cj,s}^{CES}(t) \leq p_{cj,s}^L(t) - p_{cj,s}^{PV}(t) \quad (7c)$$

Otherwise:

$$p_{cj,s}^G(t) + p_{cj,s}^{CES}(t) = p_{cj,s}^L(t) - p_{cj,s}^{PV}(t) \leq 0 \quad (8a)$$

$$p_{cj,s}^L(t) - p_{cj,s}^{PV}(t) \leq p_{cj,s}^G(t) \leq 0 \quad (8b)$$

$$p_{cj,s}^L(t) - p_{cj,s}^{PV}(t) \leq p_{cj,s}^{CES}(t) \leq 0 \quad \forall j \in \mathcal{V} \setminus \{0\}, c \in C_j, t \in \mathcal{T}, s \in \mathcal{S} \quad (8c)$$

$$p_{CES,s}^G(t) = \sum_{j=1}^N \left\{ \sum_{c \in C_j} p_{cj,s}^{CES}(t) + p_{j,s}^{CES,ch}(t) - p_{j,s}^{CES,dis}(t) \right\} \quad \forall j \in \mathcal{V} \setminus \{0\}, c \in C_j, t \in \mathcal{T}, s \in \mathcal{S} \quad (9)$$

C. Community Energy Storage Model

In this paper, we assume the CES is owned by a third party, and we designate the owner as the CES provider. The planning constraints of the CES are given by (10)-(12), and the operation of the CES is mathematically modeled by (13)-(16).

The equation (10) finds the optimal CES node, and we use a binary variable L_j , in which $L_j = 1$ suggests node j as the optimal CES node, and $L_j = 0$ means there is no CES at node j . Also, (10) guarantees only a single CES is installed in the network. The inequalities in (11) and (12) find the optimal CES capacity E_j^{cap} (in kWh) and its rated power p_j^{Rate} (in kW) at node j , respectively. Here, E_{\min}^{cap} (in kWh) and E_{\max}^{cap} (in kWh) are the minimum and maximum CES capacity limits, and p_{\max}^{Rate} is the maximum CES rated power limit.

$$\sum_{j=1}^N L_j = 1 \quad \forall j \in \mathcal{V} \setminus \{0\}, L_j \in \{0, 1\} \quad (10)$$

C. Scenario-based Stochastic Program

Since the normal and beta distributions are continuous PDFs, they represent infinite number of realizations of the random variables. Here, a realization refers to a sample real power consumption or SPV generation of a customer at a given time. A large number of realizations can model the uncertainty better at the expense of a large computational burden. But, continuous PDFs approximated as discrete functions by a finite number of realizations, as given in [15], can be used to eliminate the similar and less probable real power consumption or SPV generation values. Hence, the discretization of continuous PDFs, reduces the complexity of uncertainty modelling. Thus, both normal and beta PDFs are approximated as discrete functions by 7 realizations. Here, the approximated discrete functions are constructed to have 7 intervals, with every interval having a width of a standard deviation σ . The midpoint of an interval is a possible realization. For instance, when the forecasted real power consumption is μ , the intervals 1-7 are centered around the 7 realizations $\mu, \mu + \sigma, \mu - \sigma, \mu + 2\sigma, \mu - 2\sigma, \mu + 3\sigma$ and $\mu - 3\sigma$ as done in [16], [17]. The steps of scenario generation and reduction are given below.

- Do Step 1 to Step 5 $\forall t \in \mathcal{T}, j \in \mathcal{V} \setminus \{0\}, c \in C_j$

Step 1: Find the model parameters in (18) namely, $\sigma_{c_j}^{PV,t}$, $\alpha_{c_j}^t$ and $\beta_{c_j}^t$, by using the forecasted SPV generation $\mu_{c_j}^{PV,t}$. It is assumed that $PV_{cap,c_j} \forall j \in \mathcal{V} \setminus \{0\}, c \in C_j$ are known prior. The standard deviation $\sigma_{c_j}^{L,t}$ in (17) is taken as 4% of the mean real power consumption $\mu_{c_j}^{L,t}$ of $PDF_L(\cdot)$ [12].

Step 2: Discretize the normal and beta distributions described in (17) and (18) into 7 intervals. For this, 7 possible realizations for each PDF are calculated as $\mu, \mu + \sigma, \mu - \sigma, \mu + 2\sigma, \mu - 2\sigma, \mu + 3\sigma$ and $\mu - 3\sigma$. Then, their respective probability densities are calculated from (17) and (18). Once the probability densities are available, the probability for the occurrence of each SPV generation and real power consumption is found by taking the product of probability density and the width of each discrete interval (i.e. σ).

Step 3: Normalize the calculated probabilities of real power consumption and SPV generation. This is done by taking the sum of the probabilities, and dividing each probability by the sum [8], [16], [17]. This should be done for the 7 realizations obtained from each PDF separately. Since the continuous PDFs are approximated by discretization, sum of the 7 probabilities will only be close to unity but not exactly equal to 1. Hence, the normalization guarantees that the sum of the probabilities will be precisely equal to unity [8], [16], [17].

Step 4: Use the roulette wheel mechanism (RWM) explained in [8], [16], [17] to construct two roulette wheels in the range [0,1], each having 7 intervals. For this, assign the normalized 7 probabilities obtained from each PDF to [0,1] range. Hence, each interval has a width of the normalized probability of the respective real power consumption or SPV generation.

Step 5: Generate $N_r = |\mathcal{R}|$ number of random numbers between 0 and 1, which follow the uniform distribution. Here, the random numbers are obtained from a uniform distribution, to guarantee they are generated without any bias.

- Do Step 6 $\forall t \in \mathcal{T}, j \in \mathcal{V} \setminus \{0\}, c \in C_j, r \in \mathcal{R}$

Step 6: Assign each random number to the two roulette wheels according to their magnitudes. Select $\phi_{c_j,r}^{L,t}, \phi_{c_j,r}^{PV,t}, p_{c_j,r}^L(t)$ and $p_{c_j,r}^{PV}(t)$ from the roulette wheels corresponding to the value of the random number, where $\phi_{c_j,r}^{L,t}$ and $\phi_{c_j,r}^{PV,t}$ are the normalized probabilities of $p_{c_j,r}^L(t)$ and $p_{c_j,r}^{PV}(t)$, respectively. In this way, the initial set of scenarios are obtained.

- Do Step 7 $\forall t \in \mathcal{T}, j \in \mathcal{V} \setminus \{0\}, c \in C_j$

Step 7: A scenario reduction approach is essential in scenario based stochastic programs to keep the problem tractability, while sustaining a fair approximation for the uncertainty. Thus, the initially generated scenarios in \mathcal{R} , are then reduced to $N_s = |\mathcal{S}|$ number of scenarios to form a new scenario set \mathcal{S} , by using the K-Means clustering algorithm [8], [18]. This will generate a new set of values for the probabilities and their realizations as $\phi_{c_j,s}^{L,t}, \phi_{c_j,s}^{PV,t}, p_{c_j,s}^L(t), p_{c_j,s}^{PV}(t) \forall s \in \mathcal{S}$. The K-Means clustering method is illustrated in Algorithm 1.

Algorithm 1 K-Means Clustering Algorithm

```

1: Input  $\phi_{c_j,r}^{L,t} \forall j \in \mathcal{V} \setminus \{0\}, c \in C_j, t \in \mathcal{T}, r \in \mathcal{R}$ 
2: for each  $t$  in  $\mathcal{T}$  do
3:   for each  $j$  in  $\mathcal{V} \setminus \{0\}$  do
4:     for each  $c$  in  $C_j$  do
5:       Randomly initialize the centroids of K-Means clusters as  $Z = \{\phi_{c_j,1}^{L,t}, \dots, \phi_{c_j,s}^{L,t}, \dots, \phi_{c_j,N_s}^{L,t}\}$ , where  $|Z| = N_s$ 
6:       for each  $s$  in  $\mathcal{S}$  do
7:          $A_s \leftarrow \emptyset$ 
8:       end for
9:       while centroids of clusters do not change do
10:        for each  $r$  in  $\mathcal{R}$  do
11:           $s^* \leftarrow \underset{s}{\operatorname{argmin}} \left\| \phi_{c_j,r}^{L,t} - \phi_{c_j,s}^{L,t} \right\|$ 
12:           $A_{s^*} \leftarrow A_{s^*} \cup \{\phi_{c_j,r}^{L,t}\}$ 
13:        end for
14:        for each  $s$  in  $\mathcal{S}$  do
15:           $\phi_{c_j,s}^{L,t} \leftarrow \frac{1}{|A_s|} \sum_{\phi_{c_j,r}^{L,t} \in A_s} \phi_{c_j,r}^{L,t}$ 
16:        end for
17:        end while
18:      end for
19:    end for
20:  end for
21: Repeat Step 1 to Step 20 for the inputs  $\phi_{c_j,r}^{PV,t}, p_{c_j,r}^L(t)$  and  $p_{c_j,r}^{PV}(t)$ , separately  $\forall j \in \mathcal{V} \setminus \{0\}, c \in C_j, t \in \mathcal{T}, r \in \mathcal{R}$ 
22: Return  $\phi_{c_j,s}^{L,t}, \phi_{c_j,s}^{PV,t}, p_{c_j,s}^L(t), p_{c_j,s}^{PV}(t) \forall j \in \mathcal{V} \setminus \{0\}, c \in C_j, t \in \mathcal{T}, s \in \mathcal{S}$ 

```

- Do Step 8 $\forall t \in \mathcal{T}, s \in \mathcal{S}$

Step 8: Calculate the overall probability $\omega_{s,t}$ in (19), which gives the probability for the occurrence of scenario s at time t . The numerical values found for $\omega_{s,t}, p_{c_j,s}^L(t)$, and $p_{c_j,s}^{PV}(t) \forall j \in \mathcal{V} \setminus \{0\}, c \in C_j, t \in \mathcal{T}, s \in \mathcal{S}$ are then fed into the system models and optimization framework in Section III and V.

$$\omega_{s,t} = \frac{\left(\prod_{j=1}^N \left(\prod_{c \in C_j} \phi_{c_j,s}^{L,t} \phi_{c_j,s}^{PV,t} \right) \right)}{\sum_{s=1}^{N_s} \left(\prod_{j=1}^N \left(\prod_{c \in C_j} \phi_{c_j,s}^{L,t} \phi_{c_j,s}^{PV,t} \right) \right)} \quad (19)$$

V. MULTI-OBJECTIVE OPTIMIZATION FRAMEWORK

In this paper, it is aimed to minimize the investment cost of the CES as a planning objective, and minimize the CES operation cost and the social costs of the customers as the operation objectives. Thus, a multi-objective function is formulated by combining both planning and operation objectives.

A. Objective Functions

1) *Minimizing the Investment Cost of the CES:* The investment cost for a CES can be expressed as (20) [8], [19]. The first term of (20) relates the investment cost for the rated power of the CES, and latter for the capacity of the CES. Since minimizing the investment cost is a planning objective, it is not impacted by the uncertainty of the real power consumption and the SPV generation. Thus, (20) is independent of the scenarios.

$$f_{Inv,cost} = \rho^{CES} (C_{Rate}^{CES,Inv} p_j^{Rate} + C_{Cap}^{CES,Inv} E_j^{Cap}) \quad (20)$$

Here, $\rho^{CES} = \frac{d(1+d)^\tau}{(1+d)^\tau - 1}$, where ρ^{CES} , d , and τ are the annual cost of the CES, discount rate and the CES life time (in years), respectively. Also, $C_{Rate}^{CES,Inv}$ and $C_{Cap}^{CES,Inv}$ are the CES investment cost per kW (in *AUD/kW*) and the CES investment cost per kWh (in *AUD/kWh*), respectively.

2) *Minimizing the Operation Cost of the CES:* The cost for operating the CES is given by (21) [8]. Since (21) illustrates an operation objective, it is also a function of the scenarios.

$$f_{op,cost} = \sum_{t \in \mathcal{T}} \left(\sum_{s=1}^{N_s} \omega_{s,t} \{ C^{CES,op} p_{j,s}^{CES}(t) \} \right) \quad (21)$$

where $p_{j,s}^{CES}(t) = \eta^{ch} p_{j,s}^{CES,ch}(t) - \frac{1}{\eta^{dis}} p_{j,s}^{CES,dis}(t)$ and $C^{CES,op}$ is the CES operation cost per kW (in *AUD/kW*).

3) *Minimizing the Social Costs of the Customers:* Customers incur a cost or earn a revenue for trading energy with the CES and the grid, which is jointly named as the social costs as given in (22). Its first term denotes the energy trading cost with the grid, and latter for trading energy with the CES. Similar to (21), as the social costs of the customers is also an operation objective, $f_{C,cost}$ is a function of the scenarios.

$$f_{C,cost} = \sum_{t \in \mathcal{T}} \sum_{s=1}^{N_s} \omega_{s,t} \left\{ \lambda_G(t) \sum_{j=1}^N \sum_{c \in C_j} p_{c,j,s}^G(t) + \lambda_{CES}(t) \sum_{j=1}^N \sum_{c \in C_j} p_{c,j,s}^{CES}(t) \right\} \Delta t \quad (22)$$

Here, $\lambda_G(t)$ and $\lambda_{CES}(t)$ are the grid energy price and CES provider's energy price at time t , respectively. We adopt a one-for-one non-dispatchable energy buyback method for $\lambda_G(t)$, to value energy imports and exports from/to the grid equally [20].

B. Optimization Problem

The three objective functions which determine the CES planning and its operation, are combined together to form a multi-objective function as given in (23). The objective functions are normalized by their corresponding nadir and utopia points to attain a Pareto optimal solution for each objective compatible with the weights assigned for them [21].

$$\mathbf{x}^* = \underset{\mathbf{x} \in X}{\operatorname{argmin}} \quad w_1 \left\{ \frac{f_{Inv,cost} - f_{Inv,cost}^{utopia}}{f_{Inv,cost}^{Nadir} - f_{Inv,cost}^{utopia}} \right\} + w_2 \left\{ \frac{f_{op,cost} - f_{op,cost}^{utopia}}{f_{op,cost}^{Nadir} - f_{op,cost}^{utopia}} \right\} + w_3 \left\{ \frac{f_{C,cost} - f_{C,cost}^{utopia}}{f_{C,cost}^{Nadir} - f_{C,cost}^{utopia}} \right\} \quad (23)$$

Here,

$$\mathbf{x} = (\mathbf{L}_j, \mathbf{p}_j^{Rate}, \mathbf{E}_j^{Cap}, \mathbf{p}_j^{CES,ch}, \mathbf{p}_j^{CES,dis}, \mathbf{p}_{cj}^{CES}, \mathbf{p}_{cj}^G) \quad (24)$$

where \mathbf{x} is the decision variable vector. Here, \mathbf{L}_j , \mathbf{E}_j^{Cap} and \mathbf{p}_j^{Rate} are the vectors of the optimal CES location, CES capacity and its rated power, respectively. Vectors of the CES charging power, CES discharging power, power exchange with the CES and the grid by the customers are given by $\mathbf{p}_j^{CES,ch}$, $\mathbf{p}_j^{CES,dis}$, \mathbf{p}_{cj}^{CES} and \mathbf{p}_{cj}^G , respectively. The feasible set is given by X , which is constrained by (1)-(16). Furthermore, the calculation of the utopia and nadir values for each objective function are done in line with the techniques mentioned in [21]. Also, w_1, w_2 and w_3 are the weight coefficients of each objective function. The implementation of the overall optimization framework is succinctly given in Algorithm 2.

Algorithm 2 Algorithm to Run the Stochastic Multi-Objective Optimization

- 1: Input $\mu_{cj}^{L,t}, \mu_{cj}^{PV,t} \forall j \in \mathcal{V} \setminus \{0\}, c \in C_j, t \in \mathcal{T}$
 - 2: Initialize the model parameters used.
 - 3: Execute Step 1 to Step 8 detailed in Section IV-C, including the Algorithm 1, to model the uncertainty of the real power consumption and the SPV generation of the customers.
 - 4: Return $\omega_{s,t}, p_{cj,s}^L(t)$, and $p_{cj,s}^{PV}(t) \forall j \in \mathcal{V} \setminus \{0\}, c \in C_j, t \in \mathcal{T}, s \in \mathcal{S}$.
 - 5: Solve the multi-objective function in (23), subject to the set of constraints (1) - (16), as a MILP.
-

VI. NUMERICAL AND SIMULATION RESULTS

In the simulations, a radial distribution network with 7-nodes given in Fig. 2 was considered, and its line data can be found in [22]. The forecasted SPV generation and real power consumption data of 30 residential customers in an Australian community, for a period of 1 year, measured in 1-hour time intervals were used for simulations [23]. Here, all the residential customers generate SPV power and consume real power. Nevertheless, due to the lack of real data on customers' reactive power consumption, it was not considered for the simulations. Also, we randomly assigned the 30 customers for all the nodes except for the slack

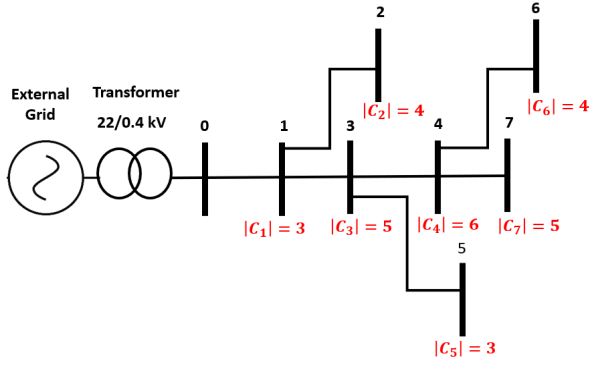


Fig. 2: The 7-Node LV radial feeder with the number of customers marked at each node

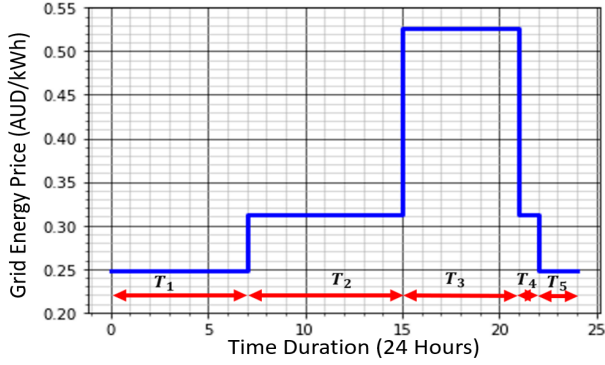


Fig. 3: Variation of the grid energy price $\lambda_G(t)$ with time

node (see Fig. 2). Therefore, $\sum_{j=1}^N |C_j| = 30$. Additionally, $|V_0| = 1p.u.$, $|V_{min}| = 0.95p.u.$, $|V_{max}| = 1.05p.u.$, $p_{max}^{Rate} = 200kW$, $E_{min}^{Cap} = 50kWh$, $E_{max}^{Cap} = 1000kWh$, $\eta^{ch} = 0.98$, $\eta^{dis} = 1.02$, $\eta_{min} = 0.05$, $\eta_{max} = 1$, $\varepsilon = 0.0001kWh$, $\Delta t = 1h$, $d = 0.1$, $\tau = 12.5$ years, $C_{Rate}^{CES,Inv} = 463AUD/kW$, $C_{Cap}^{CES,Inv} = 795AUD/kWh$ and $C_{op}^{CES,op} = 0.69AUD/kW$. Moreover, the PV capacities of the customers (i.e. PV_{cap,c_j}) were obtained from [23]. Also, the values for $C_{Rate}^{CES,Inv}$, $C_{Cap}^{CES,Inv}$ and $C_{op}^{CES,op}$ were taken assuming Li-ion as the CES technology [19].

The three objectives of the multi-objective function in (23), were weighted according to their importance. For this, we used the analytic hierarchy process (AHP) illustrated in [24]. We assigned an equal importance for $f_{Inv,cost}$ and $f_{op,cost}$, and a strong importance for $f_{C,cost}$ compared to $f_{Inv,cost}$ and $f_{op,cost}$. Therefore, the values of w_1, w_2, w_3 were calculated as $1/7, 1/7, 5/7$, respectively [24]. After computing the weight coefficients, the simulations were done over a period of 1 year (i.e. $|\mathcal{T}| = 8760$) using the CPLEX solver in Python-Pyomo.

A. Case Study I: Comparison of the Proposed Optimization Framework With its Corresponding Deterministic Model

To understand the impact of uncertainty on the optimal planning and scheduling decisions of a CES, we compared the results of the proposed stochastic optimization framework and its corresponding deterministic model. The simulations were done for our stochastic model by considering 50 initial scenarios, which is then reduced to 10 (i.e. $N_s = 10$) by using the K-Means clustering algorithm. Simulations for the deter-

ministic model were obtained by neglecting the uncertainty of real power consumption and SPV generation of the customers. The same set of constraints and the multi-objective function used for the proposed stochastic model (i.e. (1)-(16) and (23)), were used for the deterministic model as well, while excluding the scenario dependency of (1)-(9), (13)-(16) and (23).

In the simulations, a time-of-use (TOU) grid energy price $\lambda_g(t)$ shown in Fig. 3 was used [25]. Due to the lack of accurate real data about the CES provider's energy price $\lambda_{CES}(t)$, we assumed three different energy price schemes for it as (i) $\lambda_{CES}(t) = \lambda_G(t)$, (ii) $\lambda_{CES}(t) = 0$ and (iii) $\lambda_{CES}(t) = \lambda_{G,avg}$, where $\lambda_{G,avg} = \frac{\sum_{t=1}^{24} \lambda_G(t)}{24}$. A summary of the numerical results obtained for the two types of the optimization models are given in Table I. For the three energy price schemes of $\lambda_{CES}(t)$, in both deterministic and proposed stochastic models, the optimal CES location is node 7.

The p_j^{Rate} and E_j^{Cap} in the stochastic model are higher than their values in the deterministic model. In the stochastic model, due to the impact of the higher values of the realizations with respect to $\mu_{c_j}^{L,t}, \mu_{c_j}^{PV,t} \forall j \in \mathcal{V} \setminus \{0\}, c \in C_j, t \in \mathcal{T}$, both p_j^{Rate} and E_j^{Cap} will be greater than their values in the deterministic model. Moreover, in both models, the values of the planning decisions namely, L_j, p_j^{Rate} and E_j^{Cap} for their respective models have not changed irrespective of the CES provider's energy price scheme. This has happened, as the planning decisions are independent from operation variables, and thus from $\lambda_{CES}(t)$. Hence, the investment costs in the deterministic and stochastic models are AUD 32228 and 33695, respectively, irrespective of the CES provider's energy price scheme.

The operation objectives consider minimizing the CES operation cost $f_{op,cost}$, and the social costs of the customers $f_{C,cost}$. According to Table I, $f_{op,cost}$ is same for the deterministic model regardless of the CES provider's energy price scheme. This is resulted as $f_{op,cost}$ is a function independent of $\lambda_{CES}(t)$ (see (21)). Besides, when $\lambda_{CES}(t) = \lambda_G(t)$ and $\lambda_{CES}(t) = \lambda_{G,avg}(t)$, $f_{op,cost}$ in the stochastic model is higher than the corresponding deterministic model values. Since the stochastic model takes into account the uncertainty of SPV generation and real power consumption of the customers, the costs in the stochastic model are higher than the ones in the deterministic model. This behaviour is seen for $f_{C,cost}$ as well when $\lambda_{CES}(t) = \lambda_G(t)$ and $\lambda_{CES}(t) = \lambda_{G,avg}(t)$. Additionally, as $f_{C,cost} < 0$ when $\lambda_{CES}(t) = 0$, it implies that the customers earn a revenue. The customers minimize their social costs by importing power only from the CES as $\lambda_{CES}(t) = 0$. Also, the customers export power solely to the grid to maximize their social revenue. This is the intuition for $f_{C,cost}$ being negative when $\lambda_{CES}(t) = 0$ for both deterministic and stochastic models. This is discussed in detail in Section VI-B-2. In the proposed stochastic model, $f_{op,cost}$ for the three energy price schemes of $\lambda_{CES}(t)$ are different from each other. As the set of random numbers generated during stochastic modelling are unique and different for every execution of Algorithm 2, a unique set of values for $\omega_{s,t}, p_{c_j,s}^L(t)$, and $p_{c_j,s}^{PV}(t) \forall j \in \mathcal{V} \setminus \{0\}, c \in C_j, t \in \mathcal{T}, s \in \mathcal{S}$ are obtained. This results in getting different values for $f_{op,cost}$, irrespective of $f_{op,cost}$ being independent of $\lambda_{CES}(t)$.

TABLE I: RESULTS OF THE DETERMINISTIC AND PROPOSED STOCHASTIC MODELS

		Optimal CES Node L_j	Optimal CES Rated Power ¹ p_j^{Rate} (kW)	Optimal CES Capacity ¹ E_j^{Cap} (kWh)	CES Investment Cost ¹ (AUD) $f_{Inv,cost}$	CES Operation Cost ¹ (AUD) $f_{op,cost}$	Social Costs ¹ (AUD) $f_{C,cost}$
Deterministic Model	$\lambda_{CES}(t) = \lambda_G(t)$	7	72	240	32228	24674	124830
	$\lambda_{CES}(t) = 0$	7	72	240	32228	24674	-94681
	$\lambda_{CES}(t) = \lambda_{G,avg}$	7	72	240	32228	24674	70810
Proposed Stochastic Model ($N_s = 10$)	$\lambda_{CES}(t) = \lambda_G(t)$	7	78 (7.69%)	249 (3.61%)	33695 (4.35%)	27266 (9.51%)	129429 (3.55%)
	$\lambda_{CES}(t) = 0$	7	78 (7.69%)	249 (3.61%)	33695 (4.35%)	29712 (16.96%)	-98201 (3.58%)
	$\lambda_{CES}(t) = \lambda_{G,avg}$	7	78 (7.69%)	249 (3.61%)	33695 (4.35%)	29347 (15.92%)	75263 (5.92%)

¹ Increment percentage values are computed with respect to their corresponding values found in the deterministic model

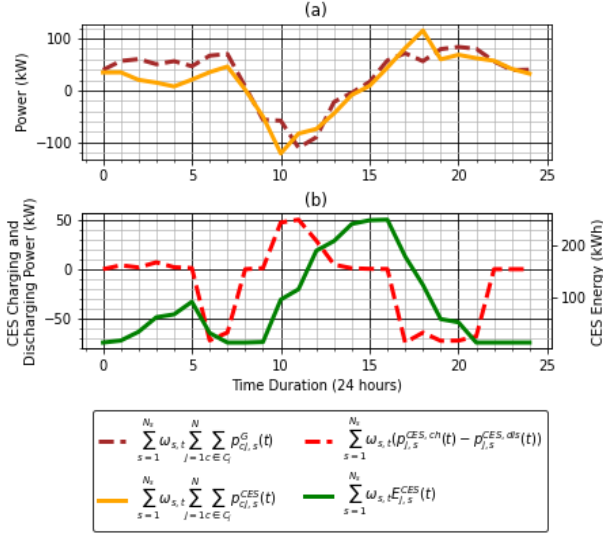


Fig. 4: (a) Total power exchange with the grid and the CES by customers, (b) CES charging/discharging power and temporal variation of CES energy - When $N_s = 10$, $\lambda_{CES}(t) = \lambda_G(t)$

B. Analysis of the Results of CES Scheduling and Mutual Power Exchanges Between the CES, the Grid and Customers

The results obtained for the proposed stochastic optimization framework, for different energy price schemes of the CES provider are detailed next. Here, we do the analysis for a randomly selected a day, for a duration of 24 hours.

1) When $\lambda_{CES}(t) = \lambda_G(t)$: Fig. 4(a) depicts the total power exchange with the grid (brown plot) and the CES (orange plot) by the customers. As the customers do not have sufficient SPV generation during T_1, T_3, T_4 and T_5 , they import power from the grid and the CES. Besides, the customers export their excess generation to the CES and the grid during T_2 . Since $\lambda_{CES}(t) = \lambda_G(t)$, the customers do not have any preference whether to exchange power with the grid or the CES. The charging and discharging pattern of the CES (red plot), and the CES energy level variation (green plot) with time are shown in Fig. 4(b). During T_1 , the CES charges, and by the end of T_1 , it discharges completely. The CES is fully discharged by the end of T_1 to exploit its full capacity to charge from the excess SPV generation during T_2 . This is evident as the CES energy level has reached its full capacity of 249 kWh during T_2 . During T_3 , the CES exports its power to the customers, and at the end of the day, CES reaches its initial energy level.

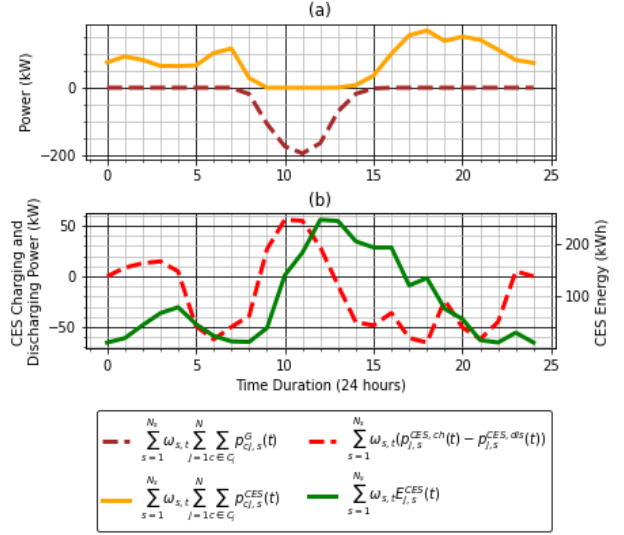


Fig. 5: (a) Total power exchange with the grid and the CES by customers, (b) CES charging/discharging power and temporal variation of CES energy - When $N_s = 10$, $\lambda_{CES}(t) = 0$

2) When $\lambda_{CES}(t) = 0$: In this case, as $\lambda_{CES}(t) = 0$, the customers neither incur a cost nor earn a revenue when trading energy with the CES. According to Fig. 5(a), during T_1 , the customers import power only from the CES, as the customers do not incur a cost for importing power from the CES. The same trend is followed by the customers during T_3, T_4 and T_5 . During T_2 , the customers export the excess SPV generation to the grid. Also, as $\lambda_{CES}(t) = 0$, the customers do not export power to the CES as they cannot earn a revenue from the CES provider. Hence, when $\lambda_{CES}(t) = 0$, the customers do not incur a cost for all time. Instead, they earn a revenue from the grid which is shown in Table I as a negative value for $f_{C,cost}$. Fig. 5(b) shows the charging and discharging pattern of the CES, including its energy level variation with time.

3) When $\lambda_{CES}(t) = \lambda_{G,avg}$: In this paper, $\lambda_{G,avg} = 0.34180$ AUD/kWh. Hence, during T_3 $\lambda_{CES}(t) < \lambda_G(t)$, and during T_1, T_2, T_4, T_5 $\lambda_{CES}(t) > \lambda_G(t)$. As seen in Fig. 6(a), during T_1 , the customers import power only from the grid. Since $\lambda_{CES}(t) > \lambda_G(t)$ during this time period, it is not economically beneficial for the customers to import expensive power from the CES. During T_2 , in which the time period with high SPV generation, the customers export the excess SPV generation to the CES as $\lambda_{CES}(t) > \lambda_G(t)$. Hence, the customers can earn a higher revenue from the CES provider.

TABLE II: RESULTS OF PROPOSED STOCHASTIC MODEL AND CASE I-IV - (WITH $N_s = 10, \lambda_{CES}(t) = \lambda_{G,avg}$)

Case / CES Node	Optimal CES Rated Power ¹ $p_j^{Rate} (kW)$	Optimal CES Capacity ¹ E_j^{Cap} (kWh)	CES Investment Cost ¹ (AUD) $f_{Inv,cost}$	CES Operation Cost ¹ (AUD) $f_{op,cost}$	Social Costs ¹ (AUD) $f_{C,cost}$	Cumulative Cost ¹ (AUD)
Proposed Model- 7 (optimal)	78	249	33695	29347	75263	138305
Case I - 3 (chosen)	124 (37.10%)	380 (34.47%)	51688 (34.81%)	44900 (34.64%)	77703 (3.14%)	174291 (20.65%)
Case II - 4 (chosen)	98 (20.41%)	303 (17.82%)	41217 (18.25%)	36723 (20.09%)	76973 (2.22%)	154913 (10.72%)
Case III - 5 (chosen)	127 (38.58%)	366 (31.97%)	50258 (32.96%)	39093 (24.93%)	77024 (2.29%)	166375 (16.87%)
Case IV - 6 (chosen)	96 (18.75%)	310 (19.68%)	41837 (19.46%)	35578 (17.51%)	76491 (1.61%)	153906 (10.14%)

¹ Increment percentage values are computed with respect to their corresponding values found in the proposed model

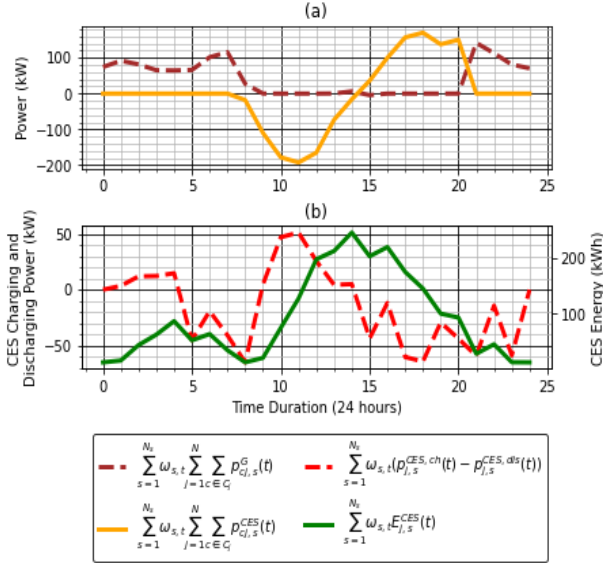


Fig. 6: (a) Total power exchange with the grid and the CES by customers, (b) CES charging/discharging power and temporal variation of CES energy - When $N_s = 10, \lambda_{CES}(t) = \lambda_{G,avg}$

Since $\lambda_{CES}(t) < \lambda_G(t)$ during T_3 , the customers import power from the CES, so that they have to pay less for the imported power. During T_4 and T_5 , the customers import power only from the grid as $\lambda_{CES}(t) > \lambda_G(t)$. Fig. 6(b) shows the charging and discharging pattern, and the temporal variation of the CES energy level with time.

C. Case Study II: Proposed Optimization Framework Vs Models With Arbitrary CES Locations

The merits of a CES may be fully exploited if its both planning and scheduling are optimized simultaneously. To test this, we compared our proposed model with four different cases that randomly choose the CES location, with $\lambda_{CES}(t) = \lambda_{G,avg}(t)$, $N_s = 10$, and taking into account the uncertainty of real power consumption and SPV generation. As given in Table II, the CES is allocated for nodes 3, 4, 5 and 6 which represent Case I, II, III and IV, respectively. For Case I-IV, we considered the constraints (1)-(16), and the objective function in (23). Additionally, $L_j = 1$ where $j \in \{3, 4, 5, 6\}$ in (10)-(12) for Case I-IV, respectively. In Case I-IV, p_j^{Rate} and E_j^{Cap} are significantly higher than in our proposed stochastic model. This has resulted in a substantial increase of the CES investment and operation costs. But,

the social costs show only a minor increase for Case I-IV compared with the increase of the investment and operation costs of the CES. This can be explained in terms of the weight coefficients used for weighting the objective functions in (20)-(22). Since w_1, w_2 and w_3 are 1/7, 1/7 and 5/7, respectively, the highest importance is given for minimizing the social costs. Hence, the optimization solver tries to maintain the social costs as much as close to $f_{C,cost}$ obtained in our proposed model. However, this comes at an expense as $f_{Inv,cost}$ and $f_{op,cost}$ which have a less significance, increase significantly. But, the cumulative cost (i.e. sum of $f_{Inv,cost}$, $f_{op,cost}$ and $f_{C,cost}$) is the least for the proposed model, while for Case I-IV, it is about 10-21% higher than the cost in our proposed model.

D. Case Study III: Impact of Scenario Reduction Approaches

In this section, we present a comparison of the results obtained for our optimization model utilizing two scenario reduction methods namely, backward scenario reduction (BSR) method and K-Means clustering algorithm. In BSR method, the initial number of scenarios are reduced by minimizing the Monge-Kantorovich distance between the scenarios in both initial and reduced scenario sets. Thereby, the initial scenarios are eliminated iteratively one by one, until the desired number of elements in the reduced scenario set is reached. Further explanation about the BSR method can be found in [12].

In this case study, we considered $\lambda_{CES}(t) = \lambda_{G,avg}$, and the initial number of scenarios as 50. The proposed optimization framework was implemented under the two scenario reduction approaches by taking $N_s = 10$ and $N_s = 30$ for each method. The numerical results obtained for this case study are summarized in Table III. Note that, for all the cases, node 7 was recorded as the optimal CES location.

The costs for all the three objectives are the highest for the model which did not use a scenario reduction method. This is because, the model with $N_s = 50$ captures more uncertainty of the real power consumption and SPV generation, so that the optimal CES rated power and the capacity are higher than the models with a lesser number of scenarios. For both K-Means and BSR methods, even with a different number of reduced scenarios (i.e. $N_s = 10$ and $N_s = 30$), the CES planning aspects have not changed. This occurs as the planning aspects are independent of the number of scenarios. Nevertheless, as the operation decisions are scenario dependent, the operation cost of the CES, and the customers' social costs have changed according to N_s . This trend is observed in the results obtained for the model which used the BSR method as well.

TABLE III: RESULTS FOR DIFFERENT SCENARIO REDUCTION METHODS - (WITH $\lambda_{CES}(t) = \lambda_{G,avg}$)

	No. of scenarios	Computational time ¹ (min)	Optimal CES Rated Power ¹ p_j^{Rate} (kW)	Optimal CES Capacity ¹ E_j^{Cap} (kWh)	CES Investment Cost ¹ (AUD) $f_{Inv,cost}$	CES Operation Cost ¹ (AUD) $f_{op,cost}$	Social Costs ¹ (AUD) $f_{C,cost}$
Without Scenario Reduction	$N_s = 50$	91	79	257	34573	38434	91321
K-Means Clustering Algorithm	$N_s = 10$	38 (58.24%)	78 (1.27%)	249 (3.11%)	33695 (2.54%)	29347 (23.64%)	75263 (17.58%)
	$N_s = 30$	53 (41.76%)	78 (1.27%)	249 (3.11%)	33695 (2.54%)	30019 (21.89%)	89425 (2.08%)
Backward Scenario Reduction Method	$N_s = 10$	41 (54.95%)	78 (1.27%)	250 (2.72%)	33735 (2.42%)	29785 (22.50%)	75709 (17.10%)
	$N_s = 30$	57 (37.36%)	78 (1.27%)	250 (2.72%)	33735 (2.42%)	30664 (20.22%)	89981 (1.47%)

¹ Decrement percentage values are computed with respect to their corresponding values found without scenario reduction

The models with reduced number of scenarios have converged for a solution in a lesser time than the case with $N_s = 50$. Scenario reduction methods like K-Means clustering algorithm and BSR method play a key role in reducing the computational time while maintaining the problem tractability. However, according to the results obtained for the models which used the K-Means and the BSR method, it is not conclusive to claim which scenario reduction method is better, as there is no any significant difference between the results.

VII. CONCLUSION & FUTURE WORK

In this paper, we have explored how the optimization of the planning and scheduling of a community energy storage (CES) benefit the CES provider by minimizing the CES investment and operation costs, and the customers by minimizing their social costs. The uncertainty of real power consumption and solar photovoltaic (SPV) generation of the customers have been accounted to formulate a scenario-based stochastic optimization program. To reduce the computational burden of the stochastic model, we have used the K-Means clustering algorithm. It has been shown that, both the customers and the CES provider can significantly minimize their personal costs by optimizing both the CES planning and its scheduling.

Future work includes extending the proposed model for unbalanced distribution networks, developing optimization models for networks with multiple CES, and considering the reactive power regulation capabilities of CES and SPV.

REFERENCES

- [1] M. Shaw, B. Sturmberg, C.P. Mediwaththe, H. Ransan-Cooper, D. Taylor and L. Blackhall, "Community batteries: a cost/benefit analysis," *Technical Report*, Australian National University, 2020.
- [2] C.P. Mediwaththe, and L. Blackhall, "Network-Aware Demand-Side Management Framework With A Community Energy Storage System Considering Voltage Constraints," *IEEE Trans. Power Syst.*, vol. 36, no. 2, pp. 1229–1238, 2021.
- [3] C.P. Mediwaththe, and L. Blackhall, "Community Energy Storage-based Energy Trading Management for Cost Benefits and Network Support," in *Proc. Int. Conf. Smart Grids and Energy Syst.*, 2020, pp. 516–521.
- [4] P.H. Divshali, and L. Söder, "Improving Hosting Capacity of Rooftop PVs by Quadratic Control of an LV-Central BSS," *IEEE Trans. Smart Grid*, vol. 10, no. 1, pp. 919–927, 2019.
- [5] M.J.E. Alam, K.M. Muttaqi, and D. Sutanto, "Community Energy Storage for Neutral Voltage Rise Mitigation in Four-Wire Multigrounded LV Feeders With Unbalanced Solar PV Allocation," *IEEE Trans. Smart Grid*, vol. 6, no. 6, pp. 2845–2855, 2015.
- [6] D.Q. Hung, and N. Mithulananthan, "Community energy storage and capacitor allocation in distribution systems," in *Proc. Aus. Uni. Power Eng. Conf.*, 2011, pp. 1–6.
- [7] M. Böhringer, S. Choudhury, S. Weck and J. Hanson, "Sizing and Placement of Community Energy Storage Systems using Multi-Period Optimal Power Flow," in *Proc. IEEE Mod. PowerTech*, 2021, pp. 1–6.
- [8] V.B. Pamshetti, and S.P. Singh, "Coordinated allocation of BESS and SOP in high PV penetrated distribution network incorporating DR and CVR schemes," *IEEE Syst. J.*, vol. 16, no. 1, pp. 420–430, 2022.
- [9] M. Mahmoodi, M. Shaw and L. Blackhall, "Voltage behaviour and distribution network performance with Community Energy Storage Systems and high PV uptake," in *Proc. ACM Int. Conf. Future Energy Syst.*, 2020, pp. 388–390.
- [10] W. Lin, and E. Bitar, "Decentralized stochastic control of distributed energy resources," *IEEE Trans. Power Syst.*, vol. 33, no. 1, pp. 888–900, 2017.
- [11] I. Atzeni, G. Scutari, D.P. Palomar and J.R. Fonollosa, "Demand-side management via distributed energy generation and storage optimization," *IEEE Trans. Smart Grid*, vol. 4, no. 2, pp. 866–876, 2012.
- [12] R. Zafar, J. Ravishankar, J.E. Fletcher and H.R. Pota, "Multi-Timescale Model Predictive Control of Battery Energy Storage System Using Conic Relaxation in Smart Distribution Grids," *IEEE Trans. Power Syst.*, vol. 33, no. 6, pp. 7152–7161, 2018.
- [13] Y. Xu, Z.Y. Dong, R. Zhang and D.J. Hill, "Multi-timescale coordinated voltage/var control of high renewable-penetrated distribution systems," *IEEE Trans. Power Syst.*, vol. 32, no. 6, pp. 4398–4408, 2017.
- [14] S.M.M. Bonab, and A. Rabiee, "Optimal reactive power dispatch: a review, and a new stochastic voltage stability constrained multi-objective model at the presence of uncertain wind power generation," *IET Gener. Transm. Distrib.*, vol. 11, no. 4, pp. 815–829, 2017.
- [15] C. Li, and I.E. Grossmann, "A review of stochastic programming methods for optimization of process systems under uncertainty," *Front. Chem. Eng.*, vol. 2, 2021.
- [16] J. Aghaei, M. Karami, K.M. Muttaqi, H.A. Shayanfar and A. Ahmadi, "MIP-based stochastic security-constrained daily hydrothermal generation scheduling," *IEEE Syst. J.*, vol. 9, no. 2, pp. 615–628, 2015.
- [17] N. Amjadi, J. Aghaei, and H.A. Shayanfar, "Stochastic multiobjective market clearing of joint energy and reserves auctions ensuring power system security," *IEEE Trans. Power Syst.*, vol. 24, no. 4, pp. 1841–1854, 2009.
- [18] F. Scarlatache, G. Grigoraş, G. Chicco and G. Cârţină, "Using k-means clustering method in determination of the optimal placement of distributed generation sources in electrical distribution systems," in *Proc. IEEE Int. Conf. Opti. Elect. Electron. Equip.*, 2012, pp. 953–958.
- [19] B. Zakeri, and S. Syri, "Electrical energy storage systems: A comparative life cycle cost analysis," *Renew. Sust. Rev.*, vol. 42, pp. 569–596, 2015.
- [20] J. Martin, "1-to-1 solar buyback vs solar feed-in tariffs: The economics," 2012. [Online]. Available: <https://www.solarchoice.net.au/blog/the-economics-of-a-1-to-1-solar-buyback-vs-solar-feed-in-tariffs/>
- [21] O. Grodzevich, and O. Romanko, "Normalization and other topics in multi-objective optimization," in *Fields MITACS Ind. Workshop*, 2006.
- [22] M. Zeraati, M.E. Hamedani Golshan, and J.M. Guerrero, "Distributed control of battery energy storage systems for voltage regulation in distribution networks with high pv penetration," *IEEE Trans. Smart Grid*, vol. 9, no. 4, pp. 3582–3593, 2018.
- [23] "Solar Home Electricity Data," [Online]. Available: <https://www.ausgrid.com.au/Industry/Research/Data-to-share/Solar-home-electricity-data/>
- [24] T.L. Saaty, "Decision making — the analytic hierarchy and Network Processes," *J. Syst. Sci. Syst. Eng.*, vol. 13, no. 1, pp. 1–35, 2004.
- [25] "Origin, "VIC residential energy price fact sheet," 2018." [Online]. Available: shorturl.at/gkmV5